

Dense Estimation of Surface Reflectance Properties of Objects with Interreflections

Abstract

In augmented virtuality which virtualizes real objects to construct a mixed reality environment, it is important to estimate object surface reflectance properties to render objects under arbitrary illumination conditions. The authors developed a method to estimate reflectance properties of object surfaces densely. However, it was difficult to estimate surface reflectance properties faithfully for objects with interreflections. This paper describes a new method of densely estimating non-uniform surface reflectance properties of real objects constructed of convex and concave surfaces with interreflections. We use registered range and surface color texture images obtained by a laser rangefinder. The proposed method first determines positions of light to take color images for discriminating diffuse and specular reflection components of surface reflection. Then, surface reflectance properties are estimated based on radiosity. Experiments show the usefulness of the proposed method.

1 Introduction

In constructing a mixed reality (MR) environment, it is required to obtain surface reflectance properties of virtualized real objects. For this purpose, we have conducted a research to estimate surface reflectance properties densely from range and surface texture images [3].

Object surface reflectance properties consist of diffuse and specular reflection components. The diffuse reflection component is easily observed due to its nature of reflection in omni-direction. On the other hand, it is difficult to observe the specular reflection component due to its nature of reflection within a fixed angle with respect to a viewing position, light source and object surface normal vector. Moreover, even if the specular reflection component is observed, this component cannot be estimated stably due to small values [1, 2, 4]. Our recent research has solved this problem by selecting optimum light positions to observe both components [3]. However, there still exists a problem such that interreflections are not considered.

In this paper, we take notice of the radiosity rendering method which can represent interreflections based on the transmission of radiosity (heat energy of light). Yu et al. [7] have estimated surface reflectance properties of a room from color and range data considering interreflections based on the radiosity method. They, however, assume that almost all objects have the same reflectance properties, therefore, their algorithm cannot be applied to an object which has non-uniform surface reflectance properties.

We propose a new method for estimating non-uniform reflectance properties of objects with interreflections to represent virtualized objects photo-realistically. The proposed method can observe the specular reflection component densely considering interreflections based on radiosity.

2 Estimation of reflectance parameters from range and color images

Figure 1 shows a flow diagram of estimating surface reflectance properties. Our process consists of three parts, which are a measurement of an object (A,C), a selection of light source (B), and an estimation of reflectance parameters (D).

2.1 Measurement of object

We use a laser rangefinder (Cyberware 3030RGB) with known positions of point light sources and a camera for acquiring surface color images, as illustrated in Figure 2(a). This system can obtain registered range and surface color texture images at the same time by rotating the rangefinder and the camera around an object, so that there is no registration error, even when an object is measured many times. Figure 2(b) shows the illustration viewed from the top of the device. A camera is located at $X1$ and a texture image is acquired through mirrors which are located at $X2$ and $X3$. We assume that the camera is virtually located at $X4$ and the camera looks toward the center of rotation.

Generally, the noise and quantization error are included in the range image acquired from the laser rangefinder. There is also a problem that it is difficult to calculate

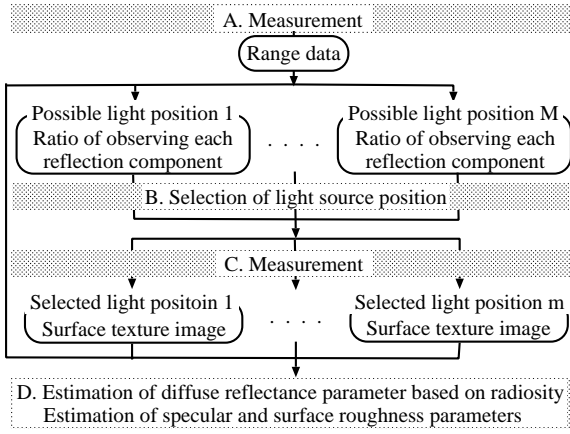


Figure 1. Flow diagram of estimating surface reflectance properties.

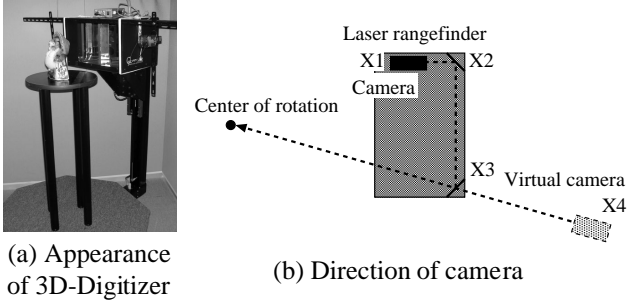


Figure 2. 3D-Digitizer.

the surface normal accurately around the discontinuity in the range image. Therefore, we employ an adaptive local quadratic surface fitting [6] as a preprocessing.

2.2 Selection of positions of light source

In the present experimental setup, multiple positions of a light are determined among 60 possible positions prepared around the laser rangefinder and these are two-dimensionally arranged at the interval of 5 cm as shown in Figure 3. The positions of a camera and a light source are calibrated in advance. When optimum light positions are selected, a single light is attached at the selected positions in turn. Therefore, the calibration of brightness among multiple lights is not needed.

Here, we employ the Torrance-Sparrow model [5] to represent object reflectance properties physically for selecting light positions. The Torrance-Sparrow model is given as:

$$i = \frac{Y}{D^2} \left\{ P_d \cos \theta_d + \frac{P_s}{\cos \theta_v} \exp\left(-\frac{\theta_r^2}{2\sigma^2}\right) \right\}, \quad (1)$$

where i represents an observed intensity, D is an attenuation coefficient concerning the distance between a point light source and an object surface point, Y represents the

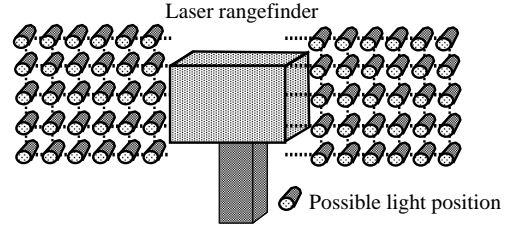


Figure 3. Multiple possible light source positions.

strength of a light source. P_d , P_s and σ are the diffuse reflectance, the specular reflectance and the surface roughness parameters, respectively. θ_d is an angle between a light source vector and a surface normal vector, θ_v is an angle between a viewing vector and a surface normal vector, and θ_r is an angle between a viewing vector and a reflection vector. Note that the reflection vector is a vector to which a light vector is mirrored against a normal vector.

To densely estimate non-uniform reflectance parameters independently, it is required to observe each pixel under three different lighting conditions: One for observing only the diffuse reflection component to determine one unknown parameter P_d and others for observing both the diffuse and specular reflection components to acquire two unknown parameters P_s and σ . Therefore, the selection of position of a light source is repeated until almost all pixels satisfies three different lighting conditions. Then, a certain number of light positions, say m , are selected to densely observe both reflection components.

2.3 Estimation of reflectance parameters

A texture image is obtained with a selected light position p ($p = 1, \dots, m$) and consists of n pixels (i_{p1}, \dots, i_{pn}), where i_{pk} means a color intensity. Each pixel is classified into three types T_{diff} , T_{spec} and T_{none} . T_{diff} means a pixel containing only the diffuse reflection component and T_{spec} means a pixel containing strong specular reflection component. T_{none} means a pixel classified neither applies to T_{diff} nor to T_{spec} and is not used to estimate reflectance parameters.

2.3.1 Estimation of diffuse reflectance parameter based on radiosity

We assume that interreflections do not have an influence from both reflection components but only from the diffuse reflection component. Therefore, a pixel which is categorized in T_{diff} is used in the following method. In this paper, to consider interreflections, we employ the radiosity equation given as:

$$B_u = E_u + P_{du} \sum_{v=1}^{\alpha} B_v F_{uv}, \quad (2)$$

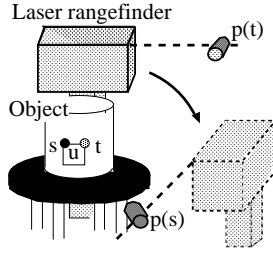


Figure 4. Calculation of radiosity.

where B_u and B_v ($1 \leq u, v \leq \alpha$) represent the radiosity of u -th and v -th patch, respectively. Note that α is the number of object patches. F_{uv} is a form factor between the patch u and the patch v . E_u is an environment term which has an influence on the patch u . In this paper, we assume that $E_u = 0$, because the object is measured in a dark room. P_{du} represents the diffuse reflectance parameter on the patch u .

In the proposed method, a form factor F_{uv} is known because the object shape is measured by the laser rangefinder. Since the range and texture images are registered at each pixel, the radiosity B_u of the patch u is calculated based on the value of the pixel which corresponds to the patch u . Then, the diffuse reflectance parameter P_{du} is estimated by Equation (2). Finally, the diffuse reflectance parameter at a each surface point is estimated by calculating the average among neighbouring patches which share the point.

Here, let $p(x)$ be the position of a light source when a pixel x is measured as shown in Figure 4, e_x be the value of the pixel x . The radiosity B_u of the patch u which includes pixels s and t is calculated by the following method. Each patch consists of four points and B_u is represented as the sum of the values of the pixels which correspond to these points. Because a light source attached with the laser rangefinder moves during measurement, it is necessary to calculate e_t with the light position $p(s)$. e_t is interpolated linearly by the following equation since e_t and e_s are categorized in T_{diff} .

$$e_t = \frac{N_t \cdot \mathbf{L}_{p(s)t}}{N_s \cdot \mathbf{L}_{p(s)s}} e_s, \quad (3)$$

where N_s and N_t are normal vectors at pixels s and t . $\mathbf{L}_{p(s)s}$ and $\mathbf{L}_{p(s)t}$ are light vectors with the light position $p(s)$ at pixels s and t . Note that in the case of $N \cdot L \leq 0$, e_t should be 0 to consider the measurability of light reflection.

2.3.2 Estimation of specular reflectance and surface roughness parameters based on Torrance-Sparrow model

The specular reflectance parameter P_{sk} and the surface roughness parameter σ_k at the k -th pixel which is categorized in T_{spec} are estimated by solving a simultaneous equation of Equation (1) with the values of the specular reflec-

tion component extracted from two images taken under two different illumination conditions and P_{dk} estimated above. See [3] for detail. Note that P_{dk} estimated above should be scaled to Equation (1) before computing the specular and surface roughness parameters.

3 Experiments

Measured objects in our experiments are shown in Figure 5(a)~(c). Object A exhibits only the diffuse reflection. On the other hand, object B and C exhibit non-uniform reflectance properties and complicated shape. For example, in object B, the leg's reflectance properties are different from the body's reflectance properties.

In a preliminary experiment, we separate the object A into two parts region A and region B. The same white paper with a uniform reflectance is pasted up on both regions. The proposed method is compared with the conventional method [3]. Results are shown in Figure 6. Each graph represents RGB channels of the diffuse reflectance parameter estimated by both methods. A horizontal axis means the position of the pixel in the vertical direction of the object and a vertical axis means the average of diffuse reflectance parameters in the horizontal direction of the object. In the conventional method, the value of the diffuse reflectance parameter is large around the boundary between regions A and B because the conventional method does not consider interreflections. On the other hand, in the proposed method, the value estimated is more stable than the value estimated by the conventional method. This clearly shows the usefulness of the proposed method.

In the next experiment, we measure objects B and C. The measurability of both reflection components and the number of selected light sources are shown in Figure 5(d). The number in the bracket means the number of selected positions of a light source required to estimate the diffuse reflectance parameter. From these results, it is observed that non-uniform surface reflectance properties are estimated over almost the whole surface considering interreflections with a limited number of light positions.

Figure 7 shows the rendering of virtualized objects B and C under virtual lighting conditions. A virtual light source moves on a circle whose center is on the vertical axis of the object. The position of the virtual light source is represented as the angle from the front of the object. The Torrance-Sparrow model is employed to render the object. Each object is rendered suitably at the part which contains interreflections. However, at the legs of object B and the lower part of object C, interreflections due to the specular reflection component cause some errors. It is necessary to eliminate such an influence.

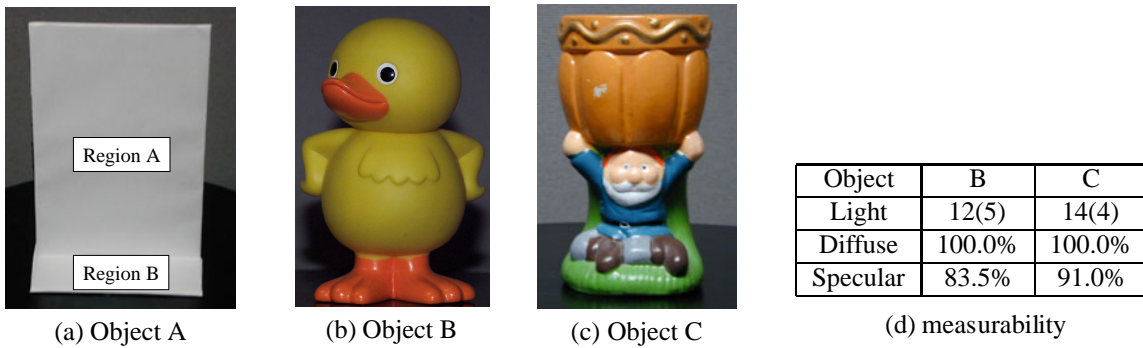


Figure 5. Three objects used in experiment and measurability of two reflection components.

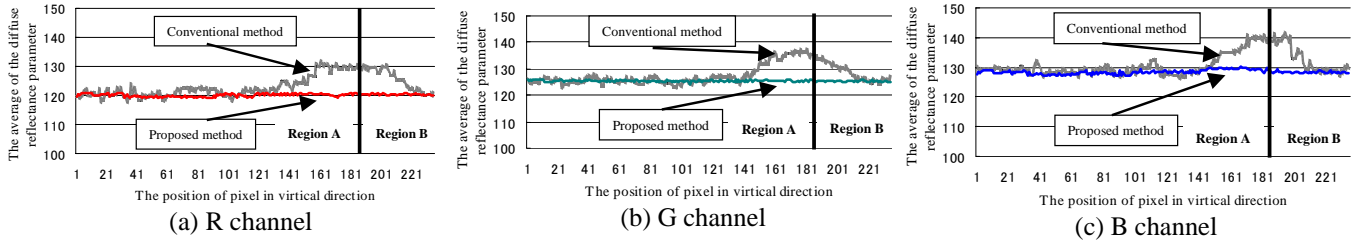


Figure 6. A comparison with previous work in a preliminary experiment.

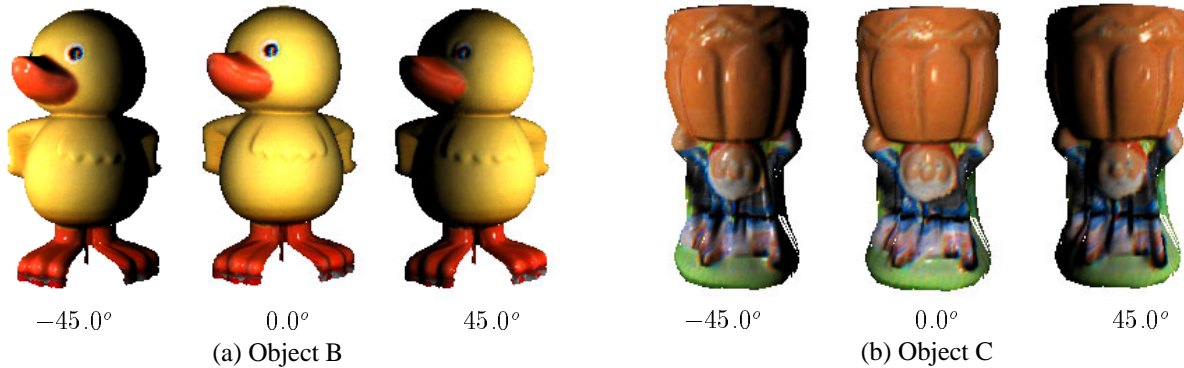


Figure 7. Rendering of virtualized objects with Torrance-Sparrow model.

4 Conclusions

In this paper, we have proposed a new method of densely estimating non-uniform reflectance properties of real objects for virtualizing the objects. In our approach, we have considered interreflections by estimating surface reflectance properties based on radiosity. The experiments have shown that the proposed method is useful for estimating the reflectance parameters of objects which exhibit non-uniform surface reflectance.

References

- [1] S. Lin and S. W. Lee. Estimation of diffuse and specular appearance. *Proc. Int. Conf. on Computer Vision*, 2:855–860, 1999.
- [2] S. Lin and S. W. Lee. A representation of specular appearance. *Proc. Int. Conf. on Computer Vision*, 2:849–854, 1999.
- [3] T. Machida, H. Takemura, and N. Yokoya. Dense estimation of surface reflectance parameters by selecting optimum illumination conditions. *Proc. Vision Interface 2001*, pages 244–251, June 2001.
- [4] Y. Sato, M. D. Wheeler, and K. Ikeuchi. Object shape and reflectance modeling from observation. *Proc. SIGGRAPH '97*, pages 379–387, 1997.
- [5] K. E. Torrance and E. M. Sparrow. Theory for off-specular reflection from roughened surfaces. *Journal of Optical Society of America*, pages 1105–1114, 1967.
- [6] N. Yokoya and M. D. Levine. Range image segmentation based on differential geometry: A hybrid approach. *IEEE Trans. Pattern Anal. Mach. Intell.*, 11(6):643–649, June 1989.
- [7] Y. Yu, P. E. Debevec, J. Malik, and T. Hawkins. Inverse global illumination: Recovering reflectance models of real scenes from photographs. *Proc. SIGGRAPH '99*, pages 215–227, August 1999.